

# Templates for homoepitaxial growth of 3C-SiC obtained by direct bonding of silicon carbide wafers of differing polytype

© M.G. Mynbaeva, D.G. Amelchuk, A.N. Smirnov, I.P. Nikitina, S.P. Lebedev,  
V.Yu. Davydov, A.A. Lebedev

Ioffe Institute,  
194021 St. Petersburg, Russia  
E-mail: mgm@mail.ioffe.ru

Received August 30, 2022

Revised November 9, 2022

Accepted November 10, 2022.

An approach of direct bonding of SiC wafers of differing polytypes has been implemented in order to create a template for cubic 3C-SiC homoepitaxy. Heteroepitaxial 3C-SiC layers grown by chemical vapor deposition were transferred onto a hexagonal 6H-SiC wafer. The results of structural characterization showed that the quality of 3C-SiC sublimation epitaxy on the templates is comparable to the level of epitaxy of cubic silicon carbide by chemical vapor deposition method. It was confirmed that the 3C-SiC layer transferred onto the 6H-SiC substrate plays the role of a crystalline „seed“ that determines cubic polytype of the overgrown SiC layer.

**Keywords:** Silicon carbide, polytypes, direct bonding, templates, sublimation epitaxy.

DOI: 10.21883/SC.2022.11.54965.9953

## 1. Introduction

The unique combination of electronic and physical properties of silicon carbide (SiC), such as a wide forbidden band, high rates of electron drift and avalanche breakdown, as well as thermal and corrosion stability, make this material a prime candidate for replacing silicon devices in the market of modern microelectronics devices [1–5].

Hexagonal polytypes 6H-SiC and 4H-SiC are used in high-power opto- and microelectronics. Single-crystal material of the 6H polytype is mainly used as a substrate material for the epitaxial growth of structures of superbright LEDs and lasers based on nitrides. High voltage power devices such as Schottky diodes and field effect transistors (FET) and metal-oxide-semiconductor FET (MOSFET) are based on 4H-SiC. The material, which is a cubic polytype 3C-SiC, is the most promising in terms of the possibility of creating based on it of efficient electronic devices with high electron mobility, in particular, for creating high-frequency field-effect transistors of MOSFET type, where, according to estimates, the mobility in the channel can reach  $380 \text{ cm}^2/(\text{V} \cdot \text{s})$ , which is unattainable for hexagonal polytypes [6]. The existing technologies for the growth of bulk SiC by the method of vapor physical transport (the modified Lely method, or the LETI method) provide the possibility of growing single crystals of only hexagonal polytypes. Carrying out high-quality 3C-SiC epitaxy on hexagonal polytype substrates is still a technological problem. Due to the discrepancy of the crystallographic symmetry under the conditions of heteropolytype epitaxy, in the grown layers formation of a large number of incoherent twin boundaries is observed [7]. The typical defects also include threading edge and screw dislocations, as well as dislocations in the base plane. The latter cause the formation

of stacking faults, which are referred to so-called „device-killing defects“, since they are the cause of degradation of devices based on SiC [8–10].

At present, for the epitaxial growth of 3C-SiC the single-crystal silicon substrates with a similar cubic crystal structure are mainly used. As growth methods, chemical vapor deposition (CVD) is used, less often — molecular beam epitaxy. This is primarily due to the fact that these methods make it possible to perform 3C-SiC epitaxy at relatively low temperatures, which makes it possible to bypass the limitation imposed by the melting temperature of Si ( $1410^\circ\text{C}$ ). The technologies of 3C-SiC heteroepitaxy on Si also have an economic advantage, which consists in the availability of large-area silicon wafers with a wide range of crystal orientations. At the same time, such technologies have a number of known problems. First of all, these include the discrepancy between parameters of the crystal lattice of 3C-SiC and Si ( $\sim 20\%$ ), and the discrepancy between the thermal expansion coefficients ( $\sim 8\%$ ). These mismatches cause the formation of crystallographic defects, as well as the bending of epitaxial structures due to occurred thermal stresses. Despite progress in the development of technologies of 3C-SiC CVD on Si, the problem of reducing the concentration of structural defects specific to the cubic SiC polytype, such as stacking faults, twins, and twin boundaries, is still relevant.

A complex solution to all the above problems can be the creation of an alternative combined substrate (template) by transferring the 3C-SiC seed layer onto a wafer of silicon carbide of hexagonal polytype. Note that at present, such transfer technologies („wafer bonding“) are widely used in epitaxial and device technologies of materials for which there is no lattice-matched substrate [11–14]. This paper reports on the creation of a combined substrate prototype

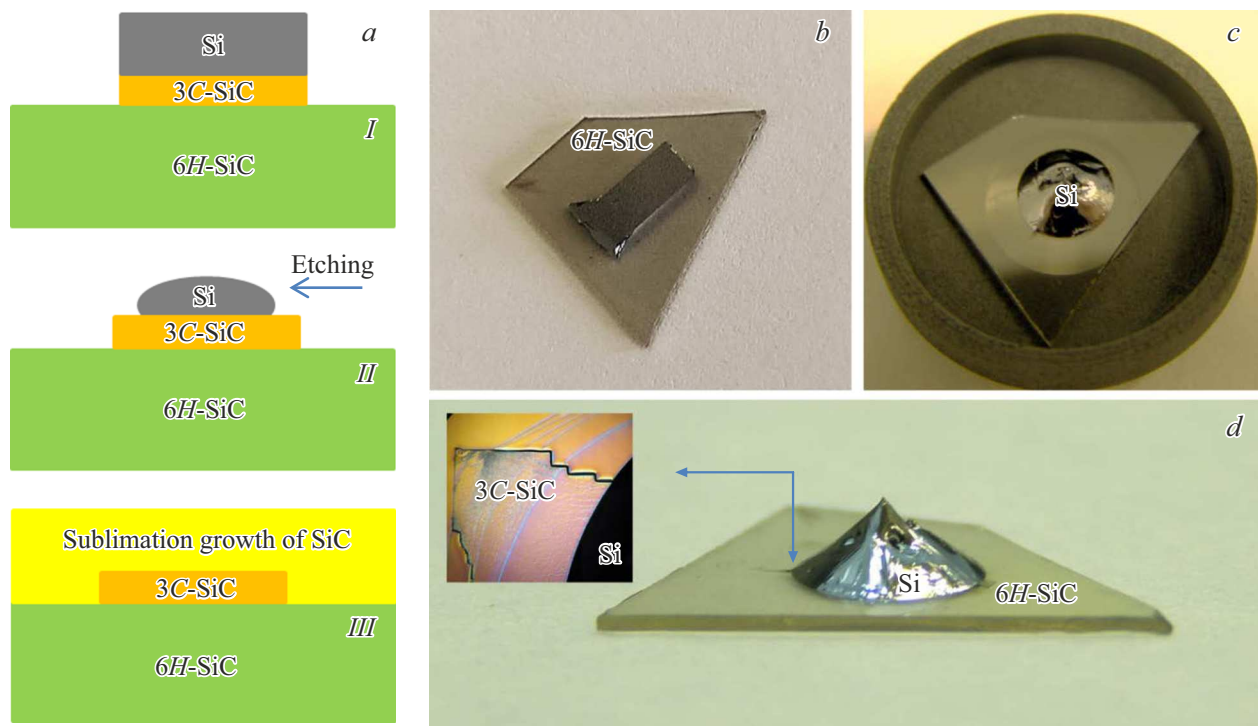


**Figure 1.** *a* — sequence of operations (I–III): I — placement of 3C-SiC/Si sample on the surface of the 6H-SiC wafer, II — vacuum annealing and Si removal, III — sublimation growth of SiC on a substrate with a transferred 3C-SiC layer; *b* — photo illustrating the initial relative position of the experimental samples; *c* — photo of the sample obtained as a result of annealing; *d* — photo of the same sample (side view). Insert — enlarged image of a part of the sample with the CVD layer 3c-SiC at the edge of the Si droplet.

by direct bonding of 3C-SiC epitaxial layers grown by the CVD method on silicon and single-crystal 6H-SiC wafers. The effectiveness of the proposed approach is confirmed by the results of sublimation homoepitaxy on the obtained 3C-SiC/6H-SiC templates.

## 2. Experiment and discussion

### 2.1. Process of manufacture

The technological processes of bonding and subsequent epitaxial growth were carried out in high-frequency induction heating unit [15]. For bonding we used 3C-SiC/Si CVD structures with epitaxial layer  $40\mu\text{m}$  thick and 6H-SiC single-crystal wafers (manufactured by LLC „Nitride Crystals“, St.Petersburg) [16]. The wafers were bound in a vacuum of  $3.0 \cdot 10^{-2}$  Torr at a temperature of  $1500^\circ\text{C}$  without using intermediate adhesive layers and without applying external mechanical pressure. The sublimation epitaxy temperature was  $1700\text{--}1800^\circ\text{C}$ , the vacuum in the growth chamber was maintained at level  $5 \cdot 10^{-6}\text{--}6 \cdot 10^{-6}$  Torr. The growth time was 1–2 h. Studies aimed at determining the structural quality of the grown layers were carried out using the methods of X-ray diffraction and Raman scattering (RS). X-ray diffraction studies were carried out on a diffractometer DRON-3 using a two-crystal spectrometer with  $\text{CuK}\alpha_1$  radiation in symmetric

Bragg reflections. A defect-free crystal 6H-SiC grown by the Lely method was used as a monochromator. The original structures 3C-SiC/Si were studied as reference samples. RS studies of the samples were carried out using a spectrometer LabRAM HR Evo UV-VIS-NIR-Open (manufactured by Horiba, France) equipped with a confocal microscope. RS spectra were recorded in backscattering geometry at room temperature. Nd:YAG laser with a wavelength of 532 nm was used as an excitation source. The focusing of the laser beam into a spot with a diameter of up to  $1\mu\text{m}$  was carried out using a  $100\times$  lens Olympus ( $\text{NA} = 0.9$ ).

Fig. 1, *a* shows a diagram of the entire technological process. Fig. 1, *b–d* shows photos of the sample before (Fig. 1, *b*) and after annealing (Fig. 1, *c* and *d*). As Figures show, annealing led to the melting of the silicon substrate and the formation of a large dome-shaped melt droplet. The insert in Fig. 1, *d* shows a microscopic image in Nomarski contrast, where one can see a part of the 3C-SiC epitaxial layer on a SiC wafer at the edge of droplet of solidified Si melt (indicated by arrows). After removing silicon in an etchant based on a mixture of nitric and hydrofluoric acids, it was found that the transferred 3C-SiC CVD layer has a mechanically strong contact with the silicon carbide substrate. Currently, experimental data confirming the formation of any adhesive layer between the bound plates were not obtained. As possible contributions to the establishment of contact, the contributions of the vapor and

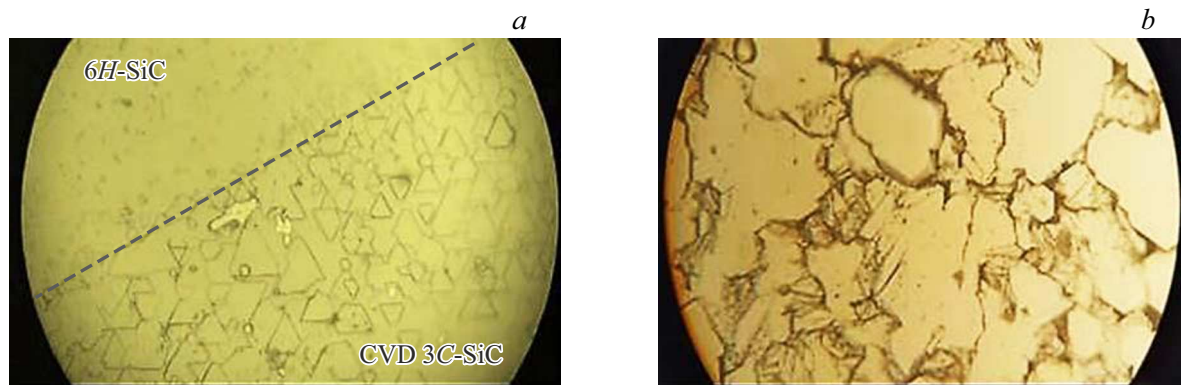


**Figure 2.** Micrographs ( $\times 500$ ): *a* — surface of sample 6H-SiC with 3C-SiC layer transferred, near its edge (indicated by dotted line), the image was obtained after removing the silicon substrate; *b* — sublimation layer 3C-SiC.

liquid phases of silicon can be considered. In particular, the contact can be formed due to the establishment of secondary chemical bonds with the participation of Si from the vapor phase, as a result of its diffusion along the boundary of the bound surfaces, and also under the action of van der Waals forces of interaction arising under conditions of hydrostatic pressure created by the liquid melt phase [17,18].

Fig. 2 shows a micrograph of the surface of 3C-SiC CVD layer transferred to the substrate obtained after the removal of the Si melt (Fig. 2, *a*), and micrograph of the surface epitaxial layer grown by the sublimation method (Fig. 2, *b*). Fig. 2, *a* shows the island nature of the structure formed at the initial stage of 3C-SiC growth on the heterosubstrate; this structure is formed by small twin formations of predominantly triangular shape [19]. On the micrograph of the surface of the sublimation layer, one can see that its structure is formed by much larger blocks, due to which the integral length of the structural boundaries separating them is significantly reduced (Fig. 2, *b*). The observed nature of the microstructure of the SiC sublimation layer testifies in favor of the fact that the island structure of the substrate determines the development of its large-block structure in accordance with the model based on the principle of self-regulation of crystal growth, originally proposed by A. van der Drift (for further discussion, see below) [20–22].

## 2.2. X-ray diffraction

The structural perfection of the investigated samples of CVD layers and sublimation layers was assessed based on the full width at half-maximum (FWHM) analysis of X-ray rocking curves recorded in the  $\omega$ -scan geometry.

For the CVD layer the obtained curves had a symmetrical Gaussian shape with the angular position of the maximum corresponding to 3C-SiC single-crystal structure. FWHM of the curves recorded on the growth surface of 3C-SiC/Si structure was 245 arcsec; from the side of the heterointerface (see Fig. 2, *a*) — 300 arcsec. Such a difference in the values of the FWHM curves reflects the known fact of the

lower quality of the crystal structure of CVD layers near the interface with the heterosubstrate [23]. Studies carried out on a series of homoepitaxial layers have shown that the quality of sublimation epitaxy on combined substrates is comparable to the quality of 3C-SiC CVD epitaxy on single-crystal silicon wafers. FWHM of the rocking curves were generally 120–170 arcsec (in some cases, when the curves were not symmetrical, their integral broadening up to 345 arcsec was observed). This fact can be explained based on the observed nature of the surface wetting of the combined substrate by the silicon melt. As seen in Fig. 1, *d*, the contact angle (wetting angle) is  $\sim 45^\circ$ . This indicates that the Si melt and the substrate react with SiC [24]. At present, the process of interaction of silicon carbide with melts is the subject of intensive studies, but its mechanism remains unclear. However, it was recently shown that at the interface between the solid and liquid phases, dissolution („etching“) of the surface of SiC wafers can occur over the entire contact area, or the interaction can be of a pronounced selective nature, when the most intense dissolution occurs in the places where structural defects appear on the SiC surface interfacing with the melt [25,26]. Note that various methods of selective etching (dry, liquid, *ex situ* and *in situ*) are successfully used in gallium nitride growth technologies in order to achieve the effect of limiting the propagation of defects contained in substrates in epitaxial layers. In particular, it was shown that pregrowth treatment of substrates makes it possible to effectively reduce the concentration of threading dislocations by 2 orders of magnitude [27–29]. Thus, it can be assumed that, due to the interaction of the silicon melt with the surface of the 3C-SiC seed crystal, changes occurred that resulted in the smoothing of the effect of its defective structure. The selective interaction could also lead to structuring of the surface of the transferred 3C-SiC crystal, as a result of which the nucleation of the blocks forming the epitaxial layer occurred on the perfect crystal planes of the twins (see Fig. 2, *a*).

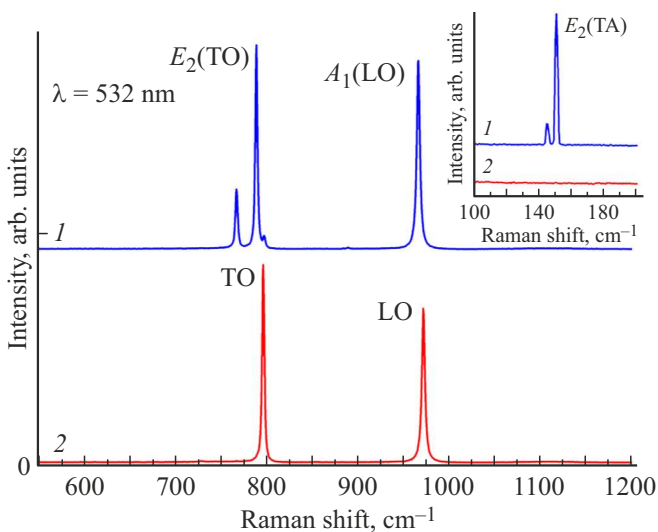


**Figure 3.** RS spectra measured in the region of the sublimation layer grown on part of the 6H-SiC wafer without the seed crystal 3C-SiC (1) and in the region of the layer on substrate with the 3C-SiC/6H-SiC (2) structure.

### 2.3. RS spectra

RS studies are used in SiC technologies as the main diagnostic method for determining the polytype of samples, the presence of other polytype inclusions in them, and evidence of polytype transformations that are possible under the influence of various external influences. It is known that in the RS spectra of 3C-SiC there are two characteristic lines corresponding to the transverse optical mode (TO) at a frequency of  $796.2\text{ cm}^{-1}$  and the longitudinal optical mode (LO) at frequency of  $972.7\text{ cm}^{-1}$  [30,31]. In the spectra of hexagonal polytypes, transverse acoustic phonons (TA) are observed, several peaks in the frequency range  $140\text{--}150$  and  $240\text{--}270\text{ cm}^{-1}$ , several TO peaks in the range  $760\text{--}800\text{ cm}^{-1}$  and peaks corresponding to LO-phonons in the range  $965\text{--}975\text{ cm}^{-1}$  (for 6H-SiC —  $967\text{ cm}^{-1}$ ) correspond to them [30,31].

Fig. 3 shows the RS spectrum (curve 1) measured in the backscattering geometry  $z(xx)\bar{z}$  (here,  $z$  axis is directed perpendicular to the substrate plane) on part of the epitaxial layer, grown in the region of the substrate without the 3C-SiC seed layer. In this case, the spectrum corresponds to the 6H-SiC hexagonal polytype, where four characteristic features are observed: LO phonon with symmetry mode  $A_1$  ( $965\text{ cm}^{-1}$ ), two phonon modes of TO symmetry  $E_2$  ( $788$  and  $766\text{ cm}^{-1}$ ), as well as two modes at frequencies  $144$  and  $150\text{ cm}^{-1}$  (see insert in Fig. 3), which correspond to transverse acoustic phonons  $E_2(\text{TA})$ . Fig. 3 also shows the RS spectrum for the layer grown on the 3C-SiC CVD layer (curve 2). The spectrum contains narrow peaks of allowed TO and LO phonon modes with frequencies of  $794$  and  $\sim 968\text{ cm}^{-1}$ , respectively. This confirms that the region under analysis corresponds to the cubic polytype. Thus, it

can be stated that it is the 3C-SiC layer transferred onto the 6H-SiC wafer that plays the role of crystalline „seed“ that determines the growth of the cubic polytype material.

### 3. Conclusion

As part of the study, the approach of direct bonding of SiC samples of various polytypes was successfully implemented. By transferring 3C-SiC heteroepitaxial CVD layers onto 6H-SiC wafer the combined 3C-SiC/6H-SiC structures were created, suitable for use as substrates for homoepitaxy of cubic polytype silicon carbide. The results obtained showed the prospects for further development of direct bonding technology to obtain full-size templates.

### Funding

This work was supported by the Russian Foundation for Basic Research (grant 20-02-00117 „Development of technology for the formation of cubic silicon carbide layers of high structural perfection“).

### Conflict of interest

The authors declare that they have no conflict of interest.

### References

- [1] T. Kimoto, J. Cooper. *Fundamentals of Silicon Carbide Technology: Growth, Characterization, Devices and Applications* (John Wiley & Sons, Ltd., Singapore, 2014).
- [2] J. Millan, P. Godignon, X. Perpina, A. Perez-Tomas, J. Rebollo. *IEEE Trans. Power Electron.*, **29**, 2155 (2014).
- [3] A. Lidow, M. de Rooij, J. Strydom, D. Reusch, J. Glaser. *GaN Transistors for Efficient Power Conversion* (John Wiley & Sons, Ltd., 2019).
- [4] F. Roccaforte, P. Fiorenza, G. Greco, R.L. Nigro, F. Gianazzo, A. Patti, M. Saggio. *Phys. Status Solidi A*, **211**, 2063 (2014).
- [5] D.G. Senesky, B. Jamshid, K.B. Chen, A.P. Pisano. *IEEE Sens. J.*, **9** (11), 1472 (2009).
- [6] S. Nishino, J.A. Powell, H.A. Will. *Appl. Phys. Lett.*, **42**, 460 (1983).
- [7] X. Li, H. Jacobson, A. Boule, D. Chaussende, A. Henrye. *ECS J. Solid State Sci. Technol.*, **3**, 75 (2014).
- [8] H. Das, S. Sunkari, J. Justice, D. Hamann. *Mater. Sci. Forum*, **1062**, 406 (2022).
- [9] J.P. Bergman, H. Lendenmann, P.A. Nilsson, U. Lindefelt, P. Skytt. *Mater. Sci. Forum*, **299**, 353 (2001).
- [10] P.C. Chen, W.C. Miao, T. Ahmed. *Nanoscale Res. Lett.*, **17**, 30 (2022).
- [11] S.H. Christiansen, R. Singh, U. Gosele. *Proc. IEEE*, **94** (12), 2060 (2006).
- [12] C. Wang, J. Xu, S. Guo, Q. Kang, Y. Wang, Y. Wang, Y. Tian. *Appl. Surf. Sci.*, **471**, 196 (2019).
- [13] Q. Kang, C. Wang, F. Niu, S. Zhou, J. Xu, Y. Tian. *Ceram. Int.*, **46**, 22718 (2020).
- [14] J. Xu, Wang, D. Li, J. Cheng, Y. Wang, C. Hang, Y. Tian. *Ceram. Int.*, **45**, 4094 (2019).

- [15] N.S. Savkina, A.A. Lebedev, A.M. Strelchuk. *Mater. Sci. Eng. B*, **77**, 50 (2000).
- [16] S.Yu. Karpov, A.V. Kulik, I.A. Zhmakin, Yu.N. Makarov, E.N. Mokhov, M.G. Ramm, M.S. Ramm, A.D. Roenkov, Yu.A. Vodakov. *J. Cryst. Growth*, **211**, 347 (2000).
- [17] T. Perham, Report of University of North Texas Libraries, UNT Digital Library.
- [18] Z.L. Liao. *Appl. Phys. Lett.*, **77** (5), 651 (2000).
- [19] R. Tu, Z. Hu, Q. Xu, L. Li, M. Yang, Q. Li, J. Shi, H. Li, S. Zhang, L. Zhang, T. Goto, H. Ohmori, M. Kosinova, B. Basu. *J. Asian Ceram. Soc.*, **7**, 312 (2019).
- [20] V. Radmilovic, U. Dahmen, D. Gao, C.R. Stoldt, C. Carraro, R. Maboudian. *Diamond. Relat. Mater.*, **16** (1), 74 (2007).
- [21] E. Spiecker, V. Radmilovic, U. Dahmen. *Acta Materialia*, **55**, (10), 3521 (2007).
- [22] A. van der Drift. *Philips Res. Rep.*, **22**, 267 (1967).
- [23] F. La Via, V. Zimbone, C. Bongiorno, A. La Magna, G. Fiscaro, I. Deretzis, V. Scuderi, C. Calabretta, F. Giannazzo, M. Zielinski, R. Anzalone, M. Mauceri, D. Crippa, E. Scalise, A. Marzegalli, A. Sarikov, L. Miglio, V. Jokubavicius, M. Syväjärvi, R. Yakimova, P. Schuh, M. Schöler, M. Kollmuss, P. Wellmann. *Materials (Basel)*, **14** (18), 5348 (2021).
- [24] H. Iyer, Y.Xiao, D. Durluk, K. Tafaghodi, K. Leili; B. Mansoor. *JOM: The journal of the Minerals, Metals & Materials Society*, **73** (1), 244 (2021).
- [25] Y. Jousseume, F. Cauwet, G. Ferro. *J. Cryst. Growth*, **593**, 126783 (2022).
- [26] S. Kawanishi, H. Shibata, T. Yoshikawa. *Materials (Basel)*, **15** (5), 1796 (2022).
- [27] M. Lee, D. Mikulik, M. Yang, S. Park. *CrystEngComm*, **19**, 2036 (2017).
- [28] W. Luo, L. Li, Z. Li, X. Xu, J. Wu, X. Liu, G. Zhang. *Appl. Surf. Sci.*, **286**, 358 (2013).
- [29] J.L. Weyher, H. Ashraf, P.R. Hageman. *Appl. Phys. Lett.*, **95** (3), 031913 (2009).
- [30] H. Okumura, E. Sakuma, J.H. Lee, H. Mukaida, S. Misawa, K. Endo, S. Yoshida. *J. Appl. Phys.*, **61** (3), 1134 (1987).
- [31] S. Nakashima, H. Harima. *Phys. Status Solidi A*, **162**, 39 (1997).